Neuron
Report

Habenula "Cholinergic" Neurons Corelease Glutamate and Acetylcholine and Activate Postsynaptic Neurons via Distinct Transmission Modes

Jing Ren,[1,2] Chang Qin,[2,3] Fei Hu,[2,3] Jie Tan,[2] Li Qiu,[4] Shengli Zhao,[4] Guoping Feng,[4,5] and Minmin Luo[2,6,*]
[1]College of Life Sciences, Beijing Normal University, Beijing 100875, China
[2]National Institute of Biological Sciences, Beijing 102206, China
[3]Graduate Program in Chinese Academy of Medical Sciences and Peking Union Medical College, Beijing 100730, China
[4]Deaprtment of Neurobiology, Duke University Medical Center, Durham, NC 27710, USA
[5]McGovern Institute for Brain Research and Department of Brain and Cognitive Sciences, Massachusetts Institute of Technology, Cambridge, MA 02139, USA
[6]School of Life Sciences, Tsinghua University, Beijing 100084, China
*Correspondence: luominmin@nibs.ac.cn
DOI 10.1016/j.neuron.2010.12.038

SUMMARY

Acetylcholine is an important neurotransmitter, and the habenulo-interpeduncular projection is a major cholinergic pathway in the brain. To study the physiological properties of cholinergic transmission in the interpeduncular nucleus (IPN), we used a transgenic mouse line in which the light-gated cation channel ChannelRhodopsin-2 is selectively expressed in cholinergic neurons. Cholinergic axonal terminals were activated by light pulses, and postsynaptic responses were recorded from IPN neurons. Surprisingly, brief photostimulation produces fast excitatory postsynaptic currents that are mediated by ionotropic glutamate receptors, suggesting wired transmission of glutamate. By contrast, tetanic photostimulation generates slow inward currents that are largely mediated by nicotinic acetylcholine receptors, suggesting volume transmission of acetylcholine. Finally, vesicular transporters for glutamate and acetylcholine are coexpressed on the same axonal terminals in the IPN. These results strongly suggest that adult brain "cholinergic" neurons can corelease glutamate and acetylcholine, but these two neurotransmitters activate postsynaptic neurons via different transmission modes.

INTRODUCTION

As a classical neurotransmitter, acetylcholine plays important signaling roles throughout the nervous system. The cholinergic system in the brain is implicated in organizing or regulating a variety of behavioral functions, such as attention, learning and memory, sleep, and arousal (Everitt and Robbins, 1997). Cholinergic neurons in the basal forebrain and brainstem provide widespread and generally diffuse projections to the cortex, thalamus, and many other brain structures (Mesulam et al., 1983). Various evidences suggest that acetylcholine is transmitted diffusively and plays mainly a modulatory role in the brain (Dani and Bertrand, 2007; Sarter et al., 2009). However, the nonspecific nature of electrical stimulation or drug application precludes the selective activation of cholinergic efferents to directly test the effects of acetylcholine transmission on postsynaptic neurons.

The projection from the medial habenula (MHb) in the epithalamus to the interpeduncular nucleus (IPN) in the midbrain represents another prominent cholinergic pathway. Anatomically, the habenulo-interpeduncular pathway is believed to serve as an important link between the limbic forebrain and the midbrain (Lecourtier and Kelly, 2007; Sutherland, 1982). Behaviorally, it is suggested to be involved in sleep, stress, pain, and nicotine addiction (Changeux, 2010; Haun et al., 1992; Hikosaka, 2010; Plenge et al., 2002; Salas et al., 2009; Sandyk, 1991).

Despite the potentially important physiological and behavioral functions of the habenulo-interpeduncular pathway, the exact physiological effects of acetylcholine transmission in the IPN remain unclear. Among phenotypically diverse neuron populations in the MHb (Andres et al., 1999; Qin and Luo, 2009; Quina et al., 2009), a majority of them expresses choline acetyltransferase (ChAT)—an enzyme that synthesizes acetylcholine (Kimura et al., 1981). Electrical stimulation of habenular efferents evokes acetylcholine release in the IPN (Sastry et al., 1979). Consistent with the finding that IPN neurons express exceptionally high levels of nicotinic acetylcholine receptors (nAChRs) (Swanson et al., 1987), external superfusion of acetylcholine and nicotine activates IPN neurons and also regulates presynaptic releases of glutamate and GABA (Brown et al., 1983; Girod et al., 2000; Léna et al., 1993; Mulle et al., 1991). However, electrical stimulation of the MHb efferents has not been reported to evoke direct postsynaptic responses that are mediated by acetylcholine receptors on IPN neurons. In contrast, this type of stimulation produces postsynaptic responses that are mediated by glutamate receptors (Brown et al., 1983; Girod and Role, 2001), paradoxically leading to the suggestion that acetylcholine is not a functional neurotransmitter for habenular cholinergic neurons (Brown et al., 1983).

To study the physiological functions of cholinergic input to IPN neurons, we require a method of selectively stimulating

exocytotic release from cholinergic synapses. Here, we took advantage of a newly developed ChAT-ChR2-EYFP BAC-transgenic mouse line, in which cholinergic neurons express the light-sensitive cation channel Channelrhodopsin-2 (ChR2) (Boyden et al., 2005; Nagel et al., 2003). By selectively stimulating cholinergic axonal terminals using optogenetics and electrophysiological recordings of postsynaptic responses from adult IPN neurons, we found that surprisingly MHb cholinergic neurons release both glutamate and acetylcholine. In addition, glutamatergic responses are fast and likely mediated by synaptic ionotropic glutamate receptors, whereas slow cholinergic effects are triggered only by tetanic stimuli and likely produced by the volume transmission of acetylcholine. These results suggest dual modes of signal transmission by cholinergic neurons in the brain.

RESULTS

Precise Optical Control of Firing Activity of MHb Cholinergic Neurons

We first tested whether ChR2-EYFP is accurately expressed in MHb cholinergic neurons of ChAT-ChR2-EYFP transgenic mice. The MHb is located in the epithalamus near the dorsal third ventricle. Its neurons project their axons to the IPN in the midbrain midline area through the fiber tract fasciculus retroflexus (fr) (Andres et al., 1999). By sectioning the mouse brain with an appropriate angle (Figure 1A), we observed strong ChR2-EYFP expression within the entire MHb-fr-IPN pathway in a single section (Figure 1B). The ventral MHb is believed to provide cholinergic output, whereas the dorsal subnucleus is considered substance P-ergic (Contestabile et al., 1987). Consistently, ChR2-EYFP expression was restricted to the ventral two-thirds of the MHb, where we also observed rich ChAT expression (Figure 1C and see Figure S1A available online). High-power view revealed that ChR2-EYFP was localized on the membrane of essentially all MHb neurons that expressed ChAT in cytoplasm (Figure 1D). We further examined the selectivity of ChR2-EYFP expression by immunostaining against vesicular acetylcholine transporter (VAChT; Figure S1B), another marker of cholinergic neurons (Arvidsson et al., 1997). ChR2-EYFP was expressed only on the cell membrane of VAChT+ neurons (Figures S1B and S1C). We also observed overlapping expression pattern of ChR2-EYFP and VAChT in neuropils and axonal fiber tracts (Figures S1B and S1C).

To examine whether transgenic expression of ChR2 effectively drives neuronal activation, we carried out whole-cell recordings from adult ChR2-EYFP+ MHb neurons in acute brain slices. Neurons were labeled to confirm their expression of ChR2-EYFP (Figure 1E). Steady blue light pulses (0.2–2 s) rapidly elicited action potential firing when cells were recorded in the current-clamp mode (Figure 1F). In the voltage-clamp mode, the same light pulses generated large inward currents (Figure 1F; peak amplitude 479 ± 93 pA; mean ± SEM; n = 14 cells). As previously demonstrated in cultured neurons (Boyden et al., 2005), light-induced currents exhibited an initial transient component that then decayed to a stable component (Figure 1F). ChR2-negative neurons in the dorsal MHb were not activated by light even at maximal light intensity (data not shown), confirming that light-evoked responses were limited to ChR2-expressing neurons.

We asked whether light stimuli can be used to control the activity of ChR2-EYFP+ cells with high temporal precision. For all 14 MHb cells tested, short light pulses (5 ms) reliably evoked firing of single action potentials in the current-clamp mode and brief large inward currents in the voltage-clamp mode (Figure 1G). In the current-clamp mode, trains of brief light flashes at different frequencies (5–50 Hz) generated precisely timed, highly reliable action potential firing (n = 8 cells tested; Figures 1H, S1D, and S1E). Thus, transgenic ChR2 expression allows us to selectively and precisely activate MHb cholinergic neurons.

Stimulation of Cholinergic Fibers Evokes Fast Glutamatergic Responses in the IPN

We next examined whether the ChAT-ChR2-EYFP mice could be used to optically stimulate cholinergic axonal terminals in the IPN (Figure S2A). Consistently with the topography of MHb-IPN projection (Contestabile et al., 1987), dense ChR2-EYFP+ terminals were localized in the core but not the peripheral region of the rostral and central IPN (Figures 2A and 2B). When viewed with high magnification, ChR2-EYFP was strongly and selectively expressed in the axonal terminals that were VAChT+ or ChAT+ (Figures 2C and S2B), suggesting accurate expression of ChR2 in cholinergic axonal terminals.

We performed whole-cell recordings from adult IPN neurons to examine the synaptic responses to optical stimulation of the cholinergic axonal terminals. Neurons were recorded and visualized to confirm their physiological properties and their location within the area targeted by ChR2-EYFP+ terminals (Figure 2D and S2C–S2E). Because a large number of GABAergic neurons were present in the IPN, we further applied a $GABA_A$-receptor blocker picrotoxin (50 μM) to isolate synaptic responses directly evoked by optical stimulation (Figure S2F).

In ~60% IPN neurons tested (n = 63/106 cells), synchronous focal activation of cholinergic fibers with brief light illumination (5 ms) evoked EPSPs and in some cases action potential firing when the cells were recorded in the current-clamp mode and fast EPSCs in the voltage-clamp mode (Figure 2E). Similar fast excitatory synaptic responses were reliably produced by a train of repetitive light pulses at 10 Hz (Figure 2F). The light intensities that were required to evoke the EPSCs were typically less than 10 mW/mm^2 (Figures S2G and S2H), which are comparable to those for activating MHb neurons. The fast EPSCs exhibited a mean peak amplitude of 111.1 ± 25.7 pA (range = [25–710] pA), a latency of 3.6 ± 0.2 ms, a rise time of 2.0 ± 0.2 ms, and a decay time constant of 5.3 ± 0.5 ms (n = 30 cells). The fast EPSCs evoked by brief light pulses resembled those evoked by single-shot electrical stimulation of the fr, within which the axons of MHb neurons traverse to the IPN (Figure S2I). The fast kinetics therefore suggests that stimulating cholinergic terminals produce fast monosynaptic EPSCs in IPN neurons. The optically-evoked EPSCs were blocked by the sodium channel blocker TTX (1 μM; Figures S2J and S2K), indicating the requirement of action potential firing within the presynaptic terminal for the generation of light-evoked EPSCs. Fast EPSCs and EPSPs were also evoked from IPN neurons by placing the optical fiber immediately

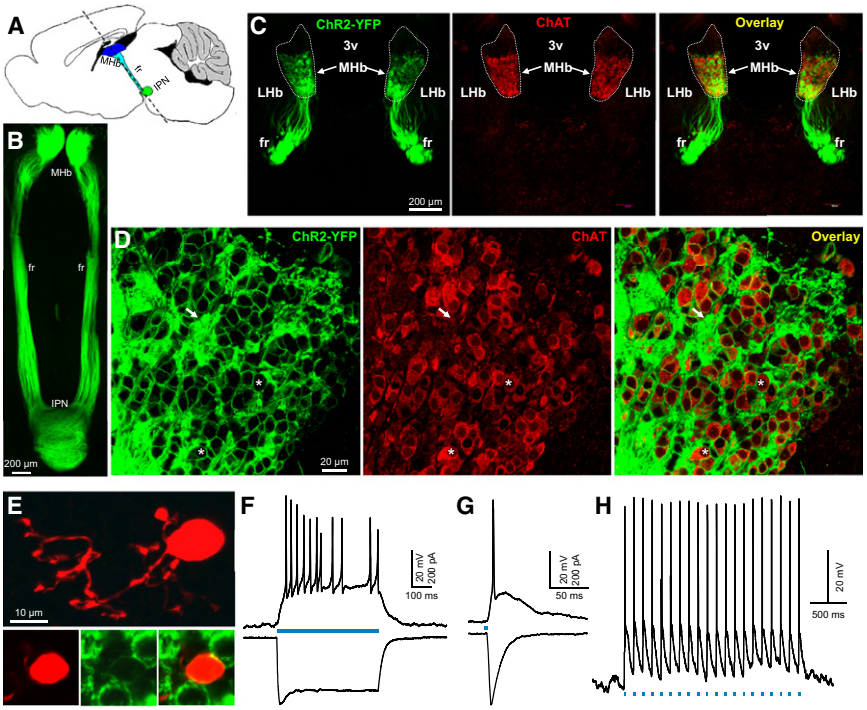

Figure 1. In ChAT-ChR2-EYFP Transgenic Mice, ChR2 Is Strongly Expressed in MHb Cholinergic Neurons and Mediates Rapid Light-Evoked Activation

(A) Schematic drawing shows the habenulo-interpeduncular projection in a sagittal plane. Dashed line indicates the angle of sectioning brain slices for physiological recordings.

(B) In ChAT-ChR2-EYFP transgenic mice, strong expression of ChR2-EYFP clearly defines the entire MHb-fr-IPN pathway.

(C) A coronal section through the epithalamus of a ChAT-ChR2-EYFP mouse shows that ChR2-EYFP (green) and ChAT (red) are strongly expressed in the ventral 2/3rd of the MHb (dashed line). 3v, dorsal 3rd ventricle; LHb, lateral habenula.

(D) Zoom-in view reveals that ChR2-EYFP (green) is localized on the membrane of cells that express ChAT (red) in the cytoplasm (see the asterisks for two examples). The arrows point to ChR2-EYFP+ neuropils that express less amounts of ChAT.

(E–J) Adult MHb cholinergic neurons can be precisely controlled with light to fire action potentials in brain slices of ChAT-ChR2-EYFP mice. (E) The morphology of a recorded cell. The claw-like dendrites are typical for MHb cells. Bottom panels show the membrane localization of ChR2-EYFP. (F) Continuous blue light illumination (500 ms; 20 mW/mm^2; blue bar) results in depolarization and action potential firing in the current-clamp mode (upper trace) and a rapid photocurrent with both transient and sustained components in the voltage-clamp mode (lower trace) (n = 14 cells). (G) A brief pulse of blue light (5 ms; blue bar) elicits an action potential in the current-clamp mode (upper trace) and a large inward photocurrent in the voltage-clamp mode (lower trace) (n = 14 cells). (H) A train of light pulses (5 ms, 10 Hz) evokes precisely timed firing of action potentials. See also Figure S1.

above MHb to selectively stimulate MHb somata (Figures 2G, 2H, and S2L), demonstrating that calcium entry through ChR2 channels in the axonal terminals is not critical for the generation of fast responses.

In the spinal cord and the peripheral nervous system, fast synaptic effects of acetylcholine are mediated by nAChRs. We applied a mixture of two nAChR antagonists (50 μM hexamethonium and 5 μM mecamylamine) to test whether the optically evoked fast EPSCs were mediated by acetylcholine transmission (Mulle et al., 1991). Surprisingly, the EPSCs were not blocked by nAChR antagonists (Figures 2I and 2J). There was a small but statistically significant increase of EPSC amplitudes in nAChR blockers, possibly because of presynaptic acetylcholine functions in the IPN (Girod et al., 2000; Girod and Role, 2001; Léna et al., 1993). However, the fast EPSCs were completely and reversibly blocked by 6,7-dinitroquinoxaline-2,3-dione (DNQX; 10 μM), a selective antagonist of AMPA-type glutamate receptor (AMPAR; Figures 2I and 2K). To examine whether NMDA receptors (NMDARs) play any role in mediating responses, we recorded EPSCs after removing the blocking action of Mg^{2+} ions. For five out of six cells tested in Mg^{2+}-free solution, DNQX application isolated a small inward current evoked by light stimulation (Figure 2L). In addition, this current was blocked by APV, an NMDAR blocker (Figures 2L and 2M). The lack of effects by nAChR blockers suggests that the EPSCs were not secondary to the released acetylcholine. More importantly, the blockade by DNQX and APV strongly suggests that brief photostimulation triggers glutamate release from cholinergic axonal terminals and produces fast monosynaptic responses that are mediated by ionotropic glutamate receptors on postsynaptic IPN neurons.

Tetanic Stimulation Evokes nAChR-Mediated Slow Responses in the IPN

We then asked whether stimulating cholinergic axonal terminals generates any direct cholinergic effect on IPN neurons. Pressure application of acetylcholine (1 mM) evoked large inward currents from IPN neurons that were reversibly abolished by nAChR blockers (Figure 3A; normalized acetylcholine amplitude = 2.5% ± 1.5% in nAChR blockers. $p < 0.001$; paired t test; n = 6 cells). Thus, as in wild-type animals (Mulle et al., 1991), acetylcholine excites IPN neurons by acting on nAChRs in ChAT-ChR2-EYFP mice.

Since brief light pulses resulted in fast EPSCs that are only mediated by glutamate receptors, we tested whether any cholinergic effects could be produced by sustained light stimuli. Continuous 5 s light pulses resulted in slowly-increasing inward currents from IPN neurons (Figure 3B). Similar slow inward currents could also be produced by prolonged stimulation using a 20 s train of light flashes (5 ms) at the frequency of ≥20 Hz (Figure 3B). Using train stimuli at 50 Hz, we observed strong inward currents from a vast majority of rostral and central IPN cells tested (n = 61/64 cells). In addition to the slow inward currents, zoom-in views reveal that the titanic photostimulation generated

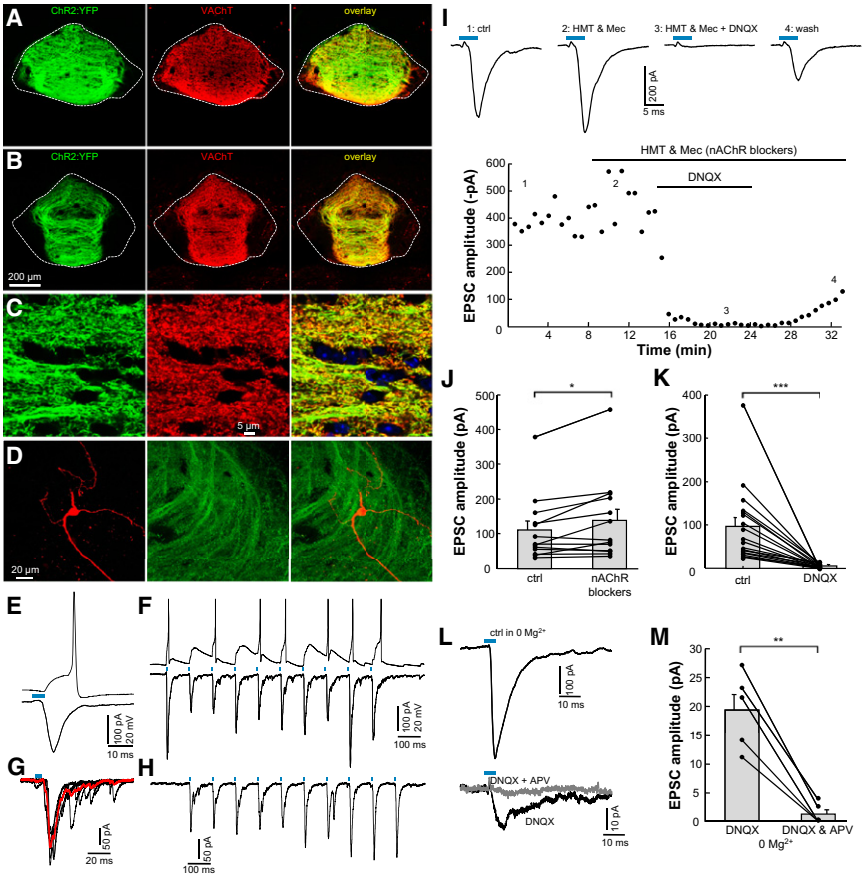

Figure 2. Activating Cholinergic Terminals by Brief Photostimulation Elicits Fast AMPAR- and NMDAR-Mediated EPSCs from IPN Neurons

(A and B) Confocal images from two coronal sections shows strong expression of ChR2-EYFP (green) and VAChT (red) within the rostral (A) and central (B) IPN (dashed lines).

(C) Zoom-in view shows that essentially all ChR2-EYFP-labeled axonal terminals (green) are immunopositive for VAChT (red) in the IPN. Blue, DAPI staining.

(D–M) Brief light illuminations elicit fast EPSCs that are mediated by ionotropic glutamate receptors but not nAChRs. (D) The morphology of an IPN neuron (red) that was located within the area covered by ChR2-EYFP+ axonal terminals (green). (E) Brief light pulse (5 ms; blue bar) elicits an EPSP and then the firing of a single action potential from an IPN neuron when recorded in the current-clamp mode (upper trace) and a fast EPSC in the voltage-clamp mode (lower trace). (F) For the same cell shown in (E), a train of 10 light pulses (5 ms, 10 Hz; blue bars) elicits EPSPs and often firings of action potentials in the current-clamp mode (upper trace) and a series of fast EPSCs in the voltage-clamp mode (lower trace). Action potentials were clipped for presentation. (G and H) Direct light stimulation of MHb somata evokes EPSCs from an IPN neuron. (G) shows the overlay of five consecutive EPSCs (black curves) and their average (red curve). Possibly because optical stimulations of MHb somata asynchronously activated axonal terminals in the IPN, the EPSCs exhibit longer latency and higher variability than those produced by terminal stimulation. (H) shows the EPSCs evoked by 10 light pulses at 10 Hz. Similar responses were observed from 6 out of 8 IPN cells tested with optical fiber placing above the MHb. (I) The fast EPSCs evoked by brief light illumination are mediated by AMPARs but not nAChRs. Synaptic stimulation caused a fast EPSC in an IPN neuron (1), which was slightly increased by the application of nAChR blockers (HMT and Mec) (2). Addition of DNQX abolished the EPSC (3), and this blockade was reversible on washout of DNQX (4). Sample traces were generated by averaging eight traces from the times indicated in the graph of EPSC amplitude versus time (lower panel). HMT, hexamethonium (50 μM); Mec, mecamylamine (5 μM). Six cells were tested with optical stimulations at the fixed intervals of 20 or 40 s. (J) Summary data show that the amplitudes of fast EPSCs are slightly increased in the presence of nAChR blockers. *$p < 0.05$ (paired t test; n = 13 cells). (K) Summary data show that the fast EPSCs are completely abolished by AMPAR antagonism. ***$p < 0.001$ (paired t test; n = 18 cells). (L) In Mg^{2+}-free solution, a brief light pulse produced a large fast EPSC from an IPN neuron (upper trace). DNQX isolated a small inward current that was then blocked by APV (lower traces). (M) Summary data show that the inward current isolated by DNQX is abolished by APV. **$p < 0.01$ (paired t test; n = 5 cells).

See also Figure S2.

many fast inward currents at high-frequency (Figure 3C, left panel). Application of DNQX blocked the fast EPSCs but did not show any effect on the slow inward currents (Figures 3C and 3D), suggesting that the fast but not slow component was mediated by glutamate receptors. In the presence of DNQX, the slow inward currents exhibited a peak amplitude of 126.9 ± 21.2 pA (range = [30–504] pA), a rise time of 15.3 ± 0.4 s, and a duration of 15.4 ± 0.8 s at half-maximum amplitude (n = 30 cells). The decay time constant was 5.0 ± 0.4 s, indicating slow recovery. In the current clamp mode, tetanic photostimulation produced depolarization and vigorous firing with gradually increasing frequency, which was only weakly reduced by DNQX during the early phase of the stimulation (Figure S3A).

Application of nAChR blockers reversibly reduced the amplitudes of the slow inward currents to about one-third of their original level (Figures 3C and 3E), indicating that a major portion of the slow currents was cholinergic in nature. In the current clamp mode, the firing evoked by tetanic photostimulation was also substantially reduced by nAChR blockers (Figure S3A). The slow responses are thus mainly mediated by nAChRs. The residual responses were not affected by the applications of atropine, (R, S)-α-Methyl-4-carboxyphenylglycine (MCPG), suramin, or APV, the blockers for muscarinic acetylcholine receptors, metabotropic glutamate receptors, P2Y purinergic receptors, and NMDA receptors, respectively (Figures S3B–S3D). The residual inward currents were unlikely the nonspecific artifact of prolonged light stimulation, as the same tetanic light stimulation failed to show any effect on IPN neurons outside of the ChR2-EYFP+ terminal field (data not shown). Tetanic light stimulations possibly trigger release of other modulatory neurotransmitters, such as peptides. Thus, the slow inward currents are most likely produced by optically triggered release of two or more neurotransmitters, with acetylcholine being the major contributor.

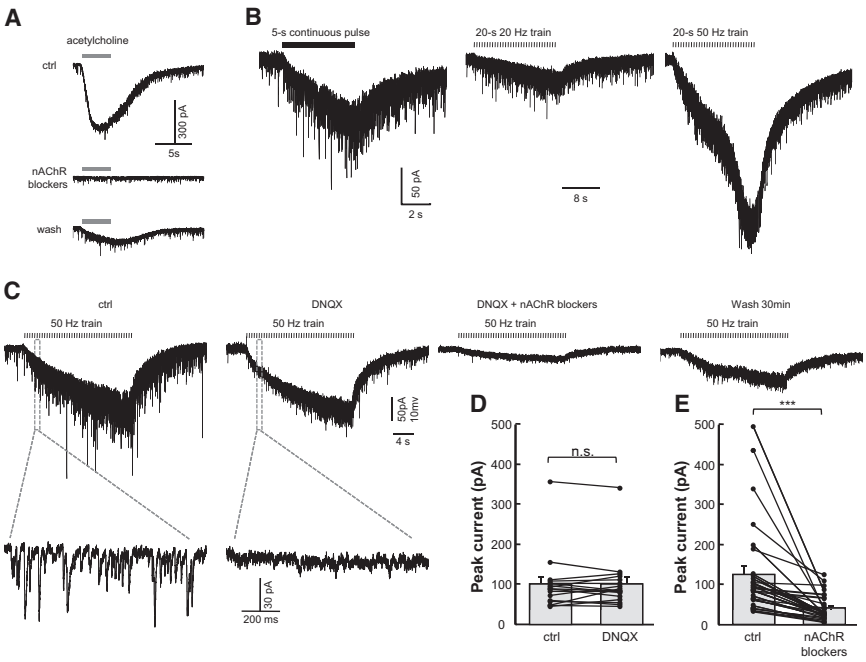

Figure 3. Tetanic Photostimulation of Axonal Terminals Produces Slow nAChR-Mediated Inward Currents from IPN Neurons

(A) Example traces from an IPN neuron show that pressure application of acetylcholine (1 mM, 4 s) produces a large inward current that is reversibly blocked by the application of nAChR blockers.

(B) Sustained photostimulation elicits slow inward currents from IPN neurons. Left panel, a slow current evoked by a 5 s continuous light pulse; middle panel, a smaller slow inward current by a 20 s train of 5 ms light pulses at 20 Hz; right panel, a much larger inward current by a 20 s train of 5 ms light pulses at 50 Hz.

(C) Example traces show that the slow component evoked by tetanic photostimulation is largely abolished by the application of nAChR blockers, whereas the fast inward currents are completely blocked by AMPAR antagonism. The slow component partially recovers after 30 min wash (right panel), suggesting reversible blockade. Traces below the left two panels show zoom-in view of the traces within the dashed boxes, illustrating that the fast component is blocked by DNQX.

(D) Group data show that the slow current evoked by tetanic photostimulation is not affected by AMPAR antagonism. n.s., nonsignificant ($p = 0.88$; paired t test; $n = 18$ cells).

(E) Group data show that the slow current is substantially reduced following nAChR blockers (***$p < 0.001$; paired t test; $n = 30$ cells).

See also Figure S3.

VGLUT1 and VAChT Are Coexpressed in Synaptic Vesicles in the IPN

Finally, we examined whether the molecular machinery exists for glutamate and acetylcholine corelease. VGLUT proteins sequester glutamate into synaptic vesicles and are considered specific markers of synapses that release glutamate as a neurotransmitter (Bellocchio et al., 2000; Fremeau et al., 2001). Our previous tract tracing and immunostaining show that many MHb neurons extend VGLUT1+ but not VGLUT2+ axonal terminals into the IPN (Qin and Luo, 2009), but it had remained unclear whether VGLUT1 is expressed in the cholinergic axonal terminals.

We tested whether VGLUT1 and VAChT are coexpressed within the same axonal terminals in the IPN by dual-color immunostainings. In wild-type C57BL/6 mice, we observed strong expression of VGLUT1 within the area occupied by VAChT+ axonal terminals (Figures 4A and 4B). Zoom-in views show that VGLUT1 and VAChT exhibited an almost identical expression pattern even at the level of axonal varicosities (Figures 4C and 4D). VGLUT1 was also expressed in noncholinergic terminals, especially in the lateral IPN where the axons of MHb noncholinergic neurons terminate (Figures 4A and 4B), suggesting that the lateral IPN receives glutamatergic but noncholinergic input. Similar expression pattern was also observed by immunostaining for VGLUT1 in ChAT-ChR2-EYFP mice (Figures S4A–S4C). VGLUT1 immunoreactivity was substantially reduced by preincubating the VGLUT1 antibody with its blocking peptide, demonstrating antibody specificity (Figure S4D).

We additionally examined whether VGLUT1 is colocalized with VAChT on synaptic vesicles by performing immunoisolations using the vesicular membrane fraction of the mouse IPN. As a control, rich VGLUT1 immunoreactivity was detected from the membrane fractions of synaptic vesicles (sv) and those immunoisolated by using antibodies to the synaptic vesicle protein synaptophysin (syp) and VGLUT1 (Figure 4E). More importantly, a substantial amount of VGLUT1 immunoreactivity was also precipitated from synaptic vesicles isolated by an antibody to VAChT (Figure 4E, rightmost lane). Reciprocally, an antibody to VGLUT1 isolated a rich amount of VAChT (Figure 4F). These immunoisolation results thus strongly indicate that VGLUT1 and VAChT are coexpressed in many synaptic vesicles in the IPN. Because VGLUT and VAChT proteins are believed to be the key components within the machinery for releasing glutamate and acetylcholine, their coexpression in the same cholinergic axonal terminals and even synaptic vesicles substantiates our physiological data showing that the axonal terminals of MHb neurons corelease glutamate and acetylcholine in the IPN.

DISCUSSION

The brain cholinergic system plays important physiological and behavioral roles. However, it had been difficult to study the physiological properties of acetylcholine transmission because of the broad, diffuse, and sparse nature of cholinergic projections. By selectively stimulating habenula cholinergic neurons using optogenetics and recording from their postsynaptic neurons in ChAT-ChR2-EYFP mice, we show that activating cholinergic axonal terminals produces fast monosynaptic excitatory responses from adult IPN neurons. These responses are blocked by antagonists of ionotropic glutamate receptors but are unaffected by

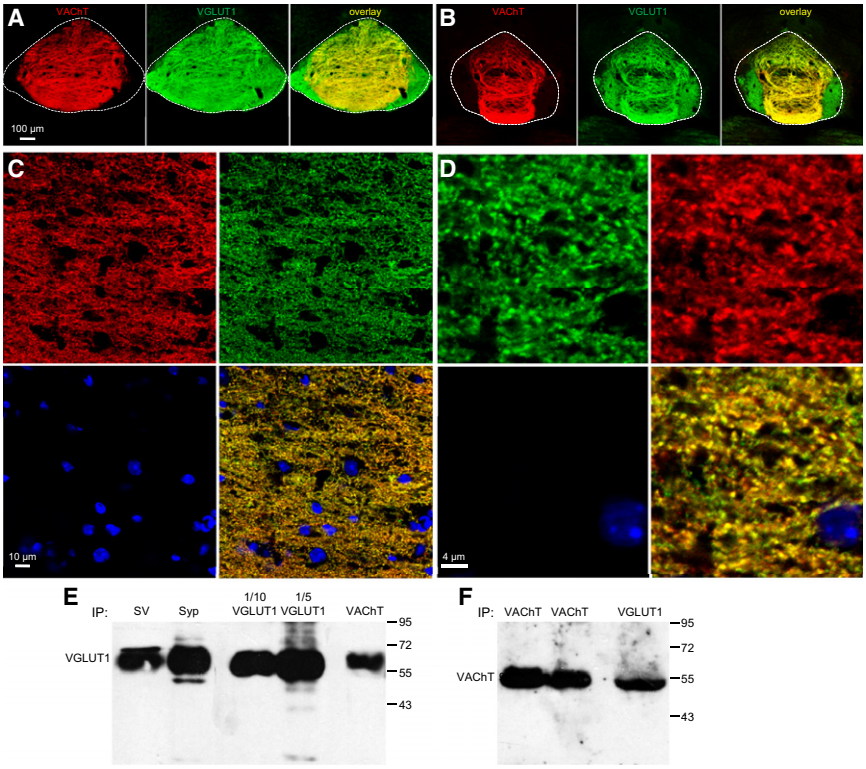

Figure 4. Cholinergic Axonal Terminals in the IPN Coexpress VGLUT1 and VAChT, Suggesting the Presence of Molecular Machinery for Glutamate and Acetylcholine Corelease

(A and B) Dual-color immunostainings show that VAChT (red) and VGLUT1 (green) are expressed within the same region in the rostral (A) and central (B) IPN of wild-type C57BL/6 mice (n = 3 mice). Images at the right of each panel show the overlay of VAChT and VGLUT1 signals.

(C) High-power view reveals strong coexpression of VAChT and VGLUT1 in the axonal terminals. Blue, DAPI labeling of cell nuclei.

(D) Zoom-in view of an area in (C) reveals an almost identical expression pattern of VAChT and VGLUT1 in axonal varicosities.

(E and F) VGLUT1 and VAChT are coexpressed in synaptic vesicles (SVs). SVs prepared from the mouse IPN were immunoprecipitated (IP) with antibodies to synaptophysin (syp), VGLUT1, or VAChT, and the isolated vesicles were then immunoblotted for VGLUT1 (E) and VAChT (F). VAChT-isolated vesicles contain VGLUT1 (E) and VGLUT1-isolated vesicles contain VAChT (F). One-tenth or one-fifth of the VGLUT1-isolated SVs was immunoblotted to avoid signal saturation in (E). Two anti-VAChT antibodies were used in (F). Numbers at right indicate MW markers (kD).

See also Figure S4.

nAChRs blockers, suggesting glutamate transmission. By immunostainings and immunoisolation of synaptic vesicles, we further show that VGLUT1 and VAChT are coexpressed in synaptic vesicles within the axonal terminals in the IPN, suggesting molecular machinery for the cotransmission of glutamate and acetylcholine. These two neurotransmitters are also co released by cultured neonatal rat forebrain neurons (Allen et al., 2006) as well as neonatal mouse spinal motoneurons and *Xenopus* tadpole spinal interneurons (Li et al., 2004; Mentis et al., 2005; Nishimaru et al., 2005), but it had remained unknown whether this corelease is limited to a specific phase during early development. Our results provide the first physiological demonstration that glutamate and acetylcholine are coreleased by adult cholinergic neurons.

The ability to generate fast EPSCs through glutamate cotransmission would allow for rapid and punctate effects that more precisely match the discharge patterns of MHb cholinergic neurons. This thus represents a mechanism for processing signals with fast kinetics to decode the information from the forebrain limbic areas to the midbrain. Several recent studies have shown that glutamate is also coreleased by neurons that have been traditionally considered to release only modulatory neurotransmitters such as serotonin and dopamine (Varga et al., 2009; Hnasko et al., 2010; Stuber et al., 2010; Tecuapetla et al., 2010). Our findings further support the concept that neurons that release modulatory, classical nonpeptide transmitters can also release glutamate to produce brief and local effects directly on their postsynaptic neurons.

Tetanic photostimulation evokes nAChR-mediated slow responses in IPN neurons, demonstrating that MHb cholinergic neurons can release acetylcholine to directly excite their postsynaptic neurons. The requirement for prolonged tetanic stimulation and the slow kinetics of cholinergic responses are consistent with the "volume transmission" model for acetylcholine. In this model, acetylcholine exerts its effects by activating extrasynaptic nAChRs after diffusing out of the synaptic cleft and/or releasing from nonsynaptic varicosities (Dani and Bertrand, 2007; Sarter et al., 2009). The volume transmission mode may explain the higher likelihood of producing slow nAChR-mediated responses using tetanic stimulation (near 100%) than evoking fast glutamatergic EPSCs using a single brief light pulse (~60%). The precise and reliable generation of monosynaptic glutamatergic EPSCs indicates "wired transmission" mode for glutamate. Many neurons failed to show glutamatergic responses to brief light pulses, possibly because they do not directly form synapses with MHb afferent terminals or their direct afferent fibers have been cut off during slice preparation. On the other hand, tetanic stimulation may release a large amount of acetylcholine that can spill over to adjacent IPN neurons. Strong synchronous firing of MHb neurons for a long period may thus recruit many IPN neurons through volume transmission of acetylcholine. In addition, the spill-over acetylcholine may also modulate both glutamatergic and GABAergic presynaptic terminals, as demonstrated by drug superfusion experiments (Girod et al., 2000; Girod and Role, 2001; Léna et al., 1993).

Despite the fact that acetylcholine transmission typically evokes rapid responses in neuromuscular junctions and the autonomic ganglia, fast cholinergic effects have been rarely observed in the mammalian brain (Dani and Bertrand, 2007). Accumulating evidences suggest the mode of volume

transmission for acetylcholine in the brain, although the degree of volume transmission or even its presence remains controversial (Dani and Bertrand, 2007; Sarter et al., 2009). Our recordings show that cholinergic responses of IPN neurons are only evoked by strong and sustained stimulation and exhibit inward currents with rise and decay time of about 10 s. This time scale is consistent with the kinetics of extracellular acetylcholine levels measured from rats performing behavioral tasks (Parikh et al., 2007). Our observations thus support the volume transmission hypothesis on the acetylcholine effect at the scale of 10 s rather than minutes or even hours.

EXPERIMENTAL PROCEDURES

Methods and materials are described in detail in Supplemental Experimental Procedures.

Animals

Adult ChAT-ChR2-EYFP mice or wild-type C57BL/6 mice of either sex (6–12 weeks old) were used. ChAT-ChR2-EYFP transgenic mice were generated by a bacterial artificial chromosome (BAC) transgenic approach.

Brain Slice Preparation and Electrophysiological Recordings

Adult ChAT-ChR2-EYFP mice were deeply anesthetized and then rapidly decapitated. Brain sections containing the MHb-fr-IPN pathway (250 μm) were cut with a vibratome and then incubated for at least 1 hr at 34°C within oxygenated aCSF. During recording, slices were submerged and superfused (2 ml/min) with aCSF at room temperature (22°C–25°C). Whole-cell recordings from the MHb or IPN were obtained under visual control of DIC microscopy.

For photostimulation, light was produced by a diode-pumped solid-state 473 nm laser or a 100 W mercury lamp. Laser light was delivered by an optical fiber (200 μm core diameter, NA = 0.22) that was submerged in aCSF and placed ~300 μm from the recording site. The light from mercury lamp passed through a 505 nm dichroic mirror and a bandwidth 460–490 nm filter and was then focused onto tissue by a 40× water immersion lens. For electrical stimulation, the fr was stimulated with a bipolar stainless steel stimulating electrode.

For drug application, DNQX (10 μM), TTX (1 μM), picrotoxin (50 μM), atropine (5 μM), MCPG (1 mM), APV (50 μM), suramin (100 μM), and a mixture of hexamethonium-Cl (50 μM) and mecamylamine (5 μM) were added to the superfusion medium by dilution of a stock solution. Acetylcholine (1 mM) was ejected with a small pressure.

Histology, Confocal Imaging, and Immunoisolation

To label neuronal morphology, cells were filled with Neurobiotin (0.25%; Vector Laboratories) and stained with Cy3-conjugated streptavidin (1:500; 2 hr) after fixation. For immunohistochemistry, coronal sections from adult mice were fixed and incubated with primary antibodies including: guinea pig anti-VGLUT1 (1:5000, 72 hr at 4°C, Millipore, AB5905), rabbit anti-VAChT (1:500, 12 hr at 4°C, Synaptic Systems), or goat anti-ChAT (1:200, 12 hr at 4°C, Millipore AB144P). After incubating with relevant flurophore-conjugated secondary antibodies, sections were mounted with DAPI-containing 50% glycerol. Images were acquired by a Zeiss 510 scanning confocal microscope (Carl Zeiss Inc.). For imaging axonal fibers at high power, a 63× oil-immersion objective (NA = 1.4) was used. Optical sections at Z axis were performed at a 0.7 μm interval.

For immunoisolation, synaptic vesicles from the IPN of adult C57BL/6 mice were isolated by a standard immunobead procedure (Hnasko et al., 2010). To coat protein G/A-Sepharose beads, we used the following antibodies: rabbit anti-VAChT (Synaptic Systems), goat anti-VAChT (Santa Cruz), guinea pig anti-VGLUT1(Millipore), and mouse anti-synaptophysin (Chemicon).

SUPPLEMENTAL INFORMATION

Supplemental Information includes four Figures and Supplemental Experimental Procedures and can be found with this article online at doi:10.1016/j.neuron.2010.12.038.

ACKNOWLEDGMENTS

This work was supported by grants from the China Ministry of Science and Technology 973 Program (2010CB833902) and 863 Program (2008AA022902) to M.L.

Accepted: November 29, 2010
Published: February 9, 2011

REFERENCES

Allen, T.G., Abogadie, F.C., and Brown, D.A. (2006). Simultaneous release of glutamate and acetylcholine from single magnocellular "cholinergic" basal forebrain neurons. J. Neurosci. *26*, 1588–1595.

Andres, K.H., von Düring, M., and Veh, R.W. (1999). Subnuclear organization of the rat habenular complexes. J. Comp. Neurol. *407*, 130–150.

Arvidsson, U., Riedl, M., Elde, R., and Meister, B. (1997). Vesicular acetylcholine transporter (VAChT) protein: a novel and unique marker for cholinergic neurons in the central and peripheral nervous systems. J. Comp. Neurol. *378*, 454–467.

Bellocchio, E.E., Reimer, R.J., Fremeau, R.T., Jr., and Edwards, R.H. (2000). Uptake of glutamate into synaptic vesicles by an inorganic phosphate transporter. Science *289*, 957–960.

Boyden, E.S., Zhang, F., Bamberg, E., Nagel, G., and Deisseroth, K. (2005). Millisecond-timescale, genetically targeted optical control of neural activity. Nat. Neurosci. *8*, 1263–1268.

Brown, D.A., Docherty, R.J., and Halliwell, J.V. (1983). Chemical transmission in the rat interpeduncular nucleus in vitro. J. Physiol. *341*, 655–670.

Changeux, J.P. (2010). Nicotine addiction and nicotinic receptors: Lessons from genetically modified mice. Nat. Rev. Neurosci. *11*, 389–401.

Contestabile, A., Villani, L., Fasolo, A., Franzoni, M.F., Gribaudo, L., Oktedalen, O., and Fonnum, F. (1987). Topography of cholinergic and substance P pathways in the habenulo-interpeduncular system of the rat. An immunocytochemical and microchemical approach. Neuroscience *21*, 253–270.

Dani, J.A., and Bertrand, D. (2007). Nicotinic acetylcholine receptors and nicotinic cholinergic mechanisms of the central nervous system. Annu. Rev. Pharmacol. Toxicol. *47*, 699–729.

Everitt, B.J., and Robbins, T.W. (1997). Central cholinergic systems and cognition. Annu. Rev. Psychol. *48*, 649–684.

Fremeau, R.T., Jr., Troyer, M.D., Pahner, I., Nygaard, G.O., Tran, C.H., Reimer, R.J., Bellocchio, E.E., Fortin, D., Storm-Mathisen, J., and Edwards, R.H. (2001). The expression of vesicular glutamate transporters defines two classes of excitatory synapse. Neuron *31*, 247–260.

Girod, R., and Role, L.W. (2001). Long-lasting enhancement of glutamatergic synaptic transmission by acetylcholine contrasts with response adaptation after exposure to low-level nicotine. J. Neurosci. *21*, 5182–5190.

Girod, R., Barazangi, N., McGehee, D., and Role, L.W. (2000). Facilitation of glutamatergic neurotransmission by presynaptic nicotinic acetylcholine receptors. Neuropharmacology *39*, 2715–2725.

Haun, F., Eckenrode, T.C., and Murray, M. (1992). Habenula and thalamus cell transplants restore normal sleep behaviors disrupted by denervation of the interpeduncular nucleus. J. Neurosci. *12*, 3282–3290.

Hikosaka, O. (2010). The habenula: from stress evasion to value-based decision-making. Nat. Rev. Neurosci. *11*, 503–513.

Hnasko, T.S., Chuhma, N., Zhang, H., Goh, G.Y., Sulzer, D., Palmiter, R.D., Rayport, S., and Edwards, R.H. (2010). Vesicular glutamate transport promotes dopamine storage and glutamate corelease in vivo. Neuron *65*, 643–656.

Kimura, H., McGeer, P.L., Peng, J.H., and McGeer, E.G. (1981). The central cholinergic system studied by choline acetyltransferase immunohistochemistry in the cat. J. Comp. Neurol. *200*, 151–201.

Lecourtier, L., and Kelly, P.H. (2007). A conductor hidden in the orchestra? Role of the habenular complex in monoamine transmission and cognition. Neurosci. Biobehav. Rev. *31*, 658–672.

Léna, C., Changeux, J.P., and Mulle, C. (1993). Evidence for "preterminal" nicotinic receptors on GABAergic axons in the rat interpeduncular nucleus. J. Neurosci. *13*, 2680–2688.

Li, W.C., Soffe, S.R., and Roberts, A. (2004). Glutamate and acetylcholine corelease at developing synapses. Proc. Natl. Acad. Sci. USA *101*, 15488–15493.

Mentis, G.Z., Alvarez, F.J., Bonnot, A., Richards, D.S., Gonzalez-Forero, D., Zerda, R., and O'Donovan, M.J. (2005). Noncholinergic excitatory actions of motoneurons in the neonatal mammalian spinal cord. Proc. Natl. Acad. Sci. USA *102*, 7344–7349.

Mesulam, M.M., Mufson, E.J., Wainer, B.H., and Levey, A.I. (1983). Central cholinergic pathways in the rat: An overview based on an alternative nomenclature (Ch1-Ch6). Neuroscience *10*, 1185–1201.

Mulle, C., Vidal, C., Benoit, P., and Changeux, J.P. (1991). Existence of different subtypes of nicotinic acetylcholine receptors in the rat habenulo-interpeduncular system. J. Neurosci. *11*, 2588–2597.

Nagel, G., Szellas, T., Huhn, W., Kateriya, S., Adeishvili, N., Berthold, P., Ollig, D., Hegemann, P., and Bamberg, E. (2003). Channelrhodopsin-2, a directly light-gated cation-selective membrane channel. Proc. Natl. Acad. Sci. USA *100*, 13940–13945.

Nishimaru, H., Restrepo, C.E., Ryge, J., Yanagawa, Y., and Kiehn, O. (2005). Mammalian motor neurons corelease glutamate and acetylcholine at central synapses. Proc. Natl. Acad. Sci. USA *102*, 5245–5249.

Parikh, V., Kozak, R., Martinez, V., and Sarter, M. (2007). Prefrontal acetylcholine release controls cue detection on multiple timescales. Neuron *56*, 141–154.

Plenge, P., Mellerup, E.T., and Wörtwein, G. (2002). Characterization of epibatidine binding to medial habenula: Potential role in analgesia. J. Pharmacol. Exp. Ther. *302*, 759–765.

Qin, C., and Luo, M. (2009). Neurochemical phenotypes of the afferent and efferent projections of the mouse medial habenula. Neuroscience *161*, 827–837.

Quina, L.A., Wang, S., Ng, L., and Turner, E.E. (2009). Brn3a and Nurr1 mediate a gene regulatory pathway for habenula development. J. Neurosci. *29*, 14309–14322.

Salas, R., Sturm, R., Boulter, J., and De Biasi, M. (2009). Nicotinic receptors in the habenulo-interpeduncular system are necessary for nicotine withdrawal in mice. J. Neurosci. *29*, 3014–3018.

Sandyk, R. (1991). Relevance of the habenular complex to neuropsychiatry: A review and hypothesis. Int. J. Neurosci. *61*, 189–219.

Sarter, M., Parikh, V., and Howe, W.M. (2009). Phasic acetylcholine release and the volume transmission hypothesis: Time to move on. Nat. Rev. Neurosci. *10*, 383–390.

Sastry, B.R., Zialkowski, S.E., Hansen, L.M., Kavanagh, J.P., and Evoy, E.M. (1979). Acetylcholine release in interpeduncular nucleus following the stimulation of habenula. Brain Res. *164*, 334–337.

Stuber, G.D., Hnasko, T.S., Britt, J.P., Edwards, R.H., and Bonci, A. (2010). Dopaminergic terminals in the nucleus accumbens but not the dorsal striatum corelease glutamate. J. Neurosci. *30*, 8229–8233.

Sutherland, R.J. (1982). The dorsal diencephalic conduction system: A review of the anatomy and functions of the habenular complex. Neurosci. Biobehav. Rev. *6*, 1–13.

Swanson, L.W., Simmons, D.M., Whiting, P.J., and Lindstrom, J. (1987). Immunohistochemical localization of neuronal nicotinic receptors in the rodent central nervous system. J. Neurosci. *7*, 3334–3342.

Tecuapetla, F., Patel, J.C., Xenias, H., English, D., Tadros, I., Shah, F., Berlin, J., Deisseroth, K., Rice, M.E., Tepper, J.M., and Koos, T. (2010). Glutamatergic signaling by mesolimbic dopamine neurons in the nucleus accumbens. J. Neurosci. *30*, 7105–7110.

Varga, V., Losonczy, A., Zemelman, B.V., Borhegyi, Z., Nyiri, G., Domonkos, A., Hangya, B., Holderith, N., Magee, J.C., and Freund, T.F. (2009). Fast synaptic subcortical control of hippocampal circuits. Science *326*, 449–453.